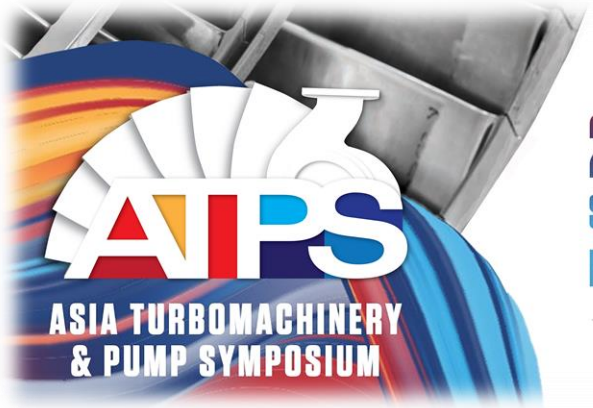

24-26 MAY 2022
SHORT COURSES: 23 MAY 2022
KUALA LUMPUR, MALAYSIA

DESIGN AND TESTING OF A CENTRIFUGAL COMPRESSOR FOR SUPERCRITICAL CO_2 APPLICATION

Alberto Milani
Systems Engineer
Baker Hughes
Florence, IT

Fulvio Bellobuono
Aerodynamic Engineer
Baker Hughes
Florence, IT

Manuele Bigi
Design Engineer
Baker Hughes
Florence, IT

Matteo Dozzini
Design Engineer
Baker Hughes
Florence, IT

Silvia Evangelisti
Testing Engineer
Baker Hughes
Florence, IT

Giuseppe Vannini
Principal Rotordymanic Engineer
Baker Hughes
Florence, IT

ABSTRACT

sCO_2Flex (Horizon 2020 grant agreement #764690) is a project that involves a consortium of several EU public and private partners. Within this program, the consortium addresses the necessities to upgrade existing fossil fuel plants to integrate renewable energy sources increasing the overall efficiency in power generation plus avoiding the use of water. Deliverable of the project is the development and validation of all main components of a sCO_2 Brayton cycle capable to provide 25MWe at 100% load ensuring a wide plant flexibility (from 100% to 20% of the electrical load). Moreover, it includes testing of a centrifugal compressor prototype.

The present work will describe several new challenges faced by original equipment manufacturer (OEM) during the design of turbomachinery for this application. The first is linked to the operating conditions of the main compressor, which achieves the highest cycle efficiency in a region close to the CO_2 critical point. In these conditions, possible co-existence of different phases may occur with sudden change of speed of sound causing uncertainties in performance predictability. To minimize these uncertainties and at the same time fulfil loop flexibility needs, specific design for compressor internals was adopted and will be discussed in this article.

The present work will conclude with highlights on the full size 5 MW prototype compressor that was manufactured and tested in OEM test facility in Q2 2021. The test replicated exactly the nominal operating conditions, specifically vicinity of the compressor suction to CO_2 critical point. This has enabled a direct validation of compressor performance predictability and at the same time allowed to verify the compressor rotordynamic, mechanics and aerodynamic behavior.

INTRODUCTION AND COMPRESSOR DESIGN

The cycle configuration selected for sCO₂Flex project is shown in Figure 1. For reference, the project data for the turbomachinery equipment is provided in [8].

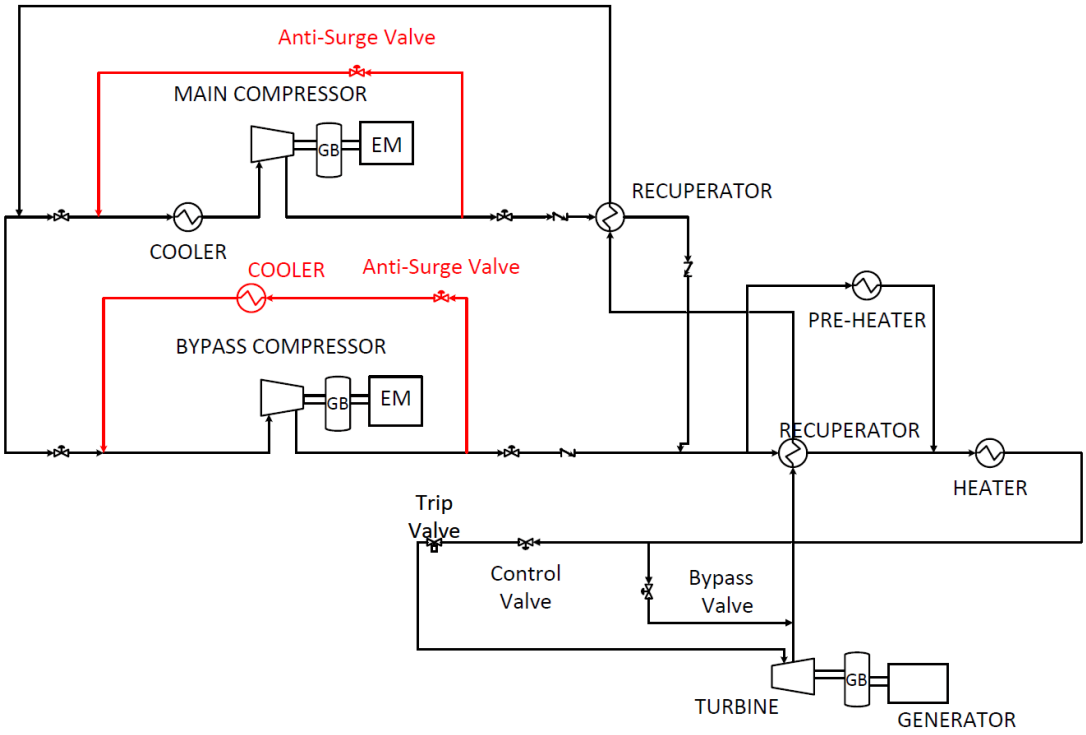

Figure 1: sCO₂Flex cycle PFD

The concept is based on a Brayton recompression cycle comprising one expander and two parallel compressor stages (Main compressor and Bypass compressor) and two heat exchanger recuperators. Main compressor suction condition is close to CO_2 critical point, which is kept stable with a heat removal unit at compressor suction, while Bypass compressor suction condition is far from the critical point.

The prototype is the Main compressor of the Brayton cycle, with suction conditions very close to CO_2 critical point (79.8 bar, 33°C, 610kg/m3) and a discharge at 250bar. The choice of compressor operating condition is a compromise between the need to maximize the cycle efficiency (reducing the compressor power) and, on the other hand, the need to keep the compressor operation within an acceptable margin with respect to saturation line (see Figure 2). Margin to saturation is evaluated considering the delta in terms of pressure and temperature between the operating point and the point that intersect the saturation line obtained considering with an iso-entropic line.

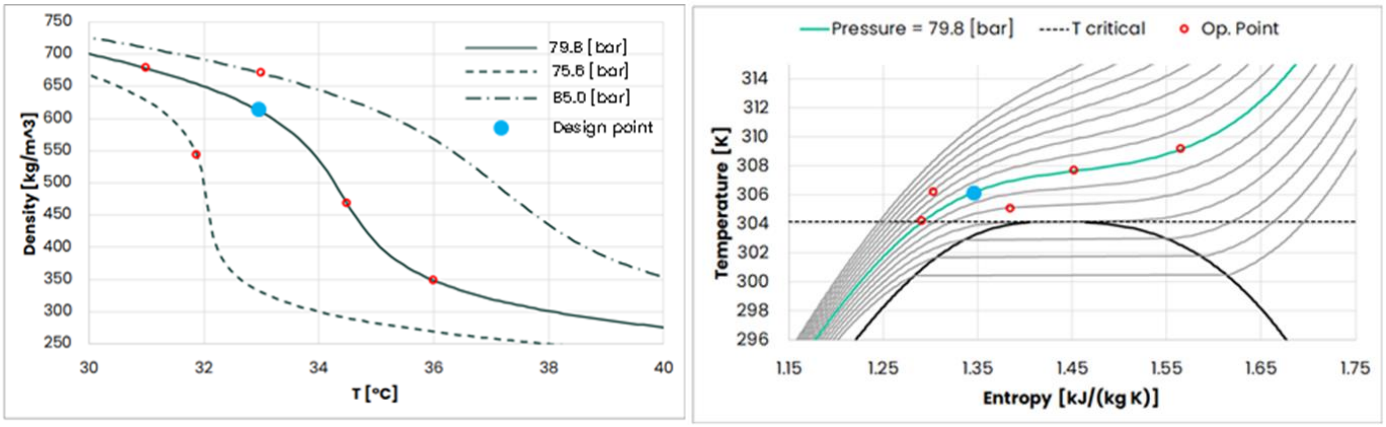

Figure 2: Density variation as function of T and CO2 diagram near critical point

It is a centrifugal compressor with a barrel casing type rating #2500, having 2 stages of 255 mm external diameter running at the rated speed of 11400 rpm and ranging from 60% to 105% speed. At the inlet the compressor is equipped with movable inlet guide vane (IGV) to guarantee a fine tuning of the suction operating condition, if required, and to achieve the required compressor flexibility in off-design conditions. The IGV blades are adjusted with a fixed first blade and a second movable blade both with a specific camber line depending on their own position. Compressor static components (suction plenum, diaphragms, and discharge volute) are forged and machined in a single piece to provide high dimensional accuracy, high-level surface roughness and eliminate split-plane leakage. The choice to machine static components in a single piece is mainly related to the small compressor dimensions. The rotor is composed by four main parts (the forward-stub shaft, the two impellers and the after-stub shaft) that are stacked and connected to each other via a tie rod (see Figure 3).

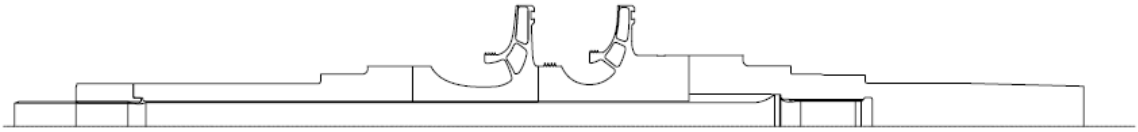

Figure 3: Stacked rotor

Torque transmission is guaranteed by the contact friction, while a low stiffness radial fitting is used for centering purpose and such to allow a cold assembly avoiding warm heating of the parts. Special care of the design of the torque transmission has been required because of the high-power density of the machine and the relatively low rotational speed resulting in a high torque requirement. For this reason, the design also includes a series of backup pins that work in case the actual torque exceeds the contact friction torque capability. Thrust collar is not integral since it must be dismantled for the removal of dry gas seals (DGS) and is shrink fitted to the forward stub shaft. The balance drum is integral to the shaft part and the seal design is a pocket damper seal. Impeller seals are teeth on rotor (TOR) type and have an abradable zone on static parts to reduce the clearance and consequently the relative leakage. The shaft end seals are tandem DGS. The first impeller has a dedicated design to cope with the CO_2 supercritical characteristics.

The prototype of the main compressor was manufactured and tested in OEM test facility in Q2 2021. The test replicated exactly the nominal operating conditions, specifically vicinity of the compressor suction to CO_2 critical point. The test achieved 125 running hours in CO2 supercritical conditions, including more than 50 start-ups. This has enabled a direct validation of compressor performance predictability and at the same time allowed to verify the compressor rotordynamic, mechanical and aerodynamic behavior.

TEST BENCH FACILITY

An existing test facility in OEM site was redesigned and upgraded to test sCO_2 prototype compressor complete operating map, varying rotating speed from 60% to 100%, and adjusting IGV openings from -60° to +10° (Figure 4). The test compressor train includes a driver (GE-10 turbine), a low-speed coupling, a gearbox, and a high-speed coupling; on the low-speed side, a torque meter provided mechanical power measurement used in transient operations for energy balance with possible presence of bi-phase fluid.

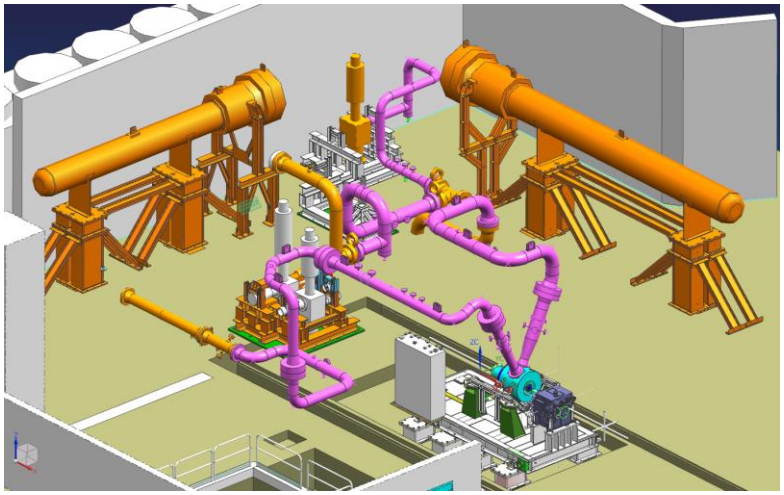

Figure 4: sCO_2Flex Test Bench

The test rig is a closed loop equipped with a shell and tube heat exchanger and pressure regulation valves. A by-pass line with an additional control valve was installed to add flexibility in compressor suction temperature regulation. The loop is provided with auxiliary systems for lube oil, cooling water and seal gas system to feed DGS. It was pressurized through a filling line capable of providing 100Bar at 60°C. An on-line heater was installed on the filling line to avoid sub cooling and liquid formation during loop loading and refilling. A vent skid with two parallel branches, one equipped with a fast-opening valve and the other with a series of two manual valves was used for loop blow down and fine tuning. All valves and downstream piping were heat traced to avoid total or partial blockage due to dry ice formation.

The test was designed in compliance with ASME PTC 10. Considering the high uncertainty on calculated density on suction, mass flow was measured by redundant orifice plates in accordance with ISO5167 both on suction and on discharge, where density dependence on temperature is reduced and overall uncertainty on mass flow is lower. The control system main target was to maintain compressor suction condition as per design point 79.8 bar, 33+/-0.1°C to avoid unintended CO_2 liquid phase conditions. The main challenge was the strict tolerance on suction temperature, required because of the large gradients of the thermodynamic properties associated to small Delta T close to the critical point (see Figure 2). A controllability simulation was performed to assess control system ability to manage tight tolerance on inlet conditions in all tested operating conditions and to manage transient conditions while keeping away from liquid conditions. Temperature control was obtained by automatic tuning of a set of two control valves on cooling water system, regulating water flow to the cooler; in addition, a second control for fine adjustment was set on the by-pass valve diverting part of the flow from the heat exchanger, for quickly increasing temperature when operating close to condensation line. In addition, simulations were carried out to verify loop operability in all the off-design conditions of interest.

Specific process simulations were executed on pressure safety valves on process gas and dry gas seal vents: results showed that, with sections increasingly blocked by ice formation, a sufficient passage area remains free from dry ice due to erosional speed, guaranteeing functionality in all conditions. The assessment also involved mechanical equipment geometry and materials selection. The pilot-operated PSV was heat traced to minimize solid CO_2; supports were designed against valve opening force. Performance was elaborated real time by a tailored proprietary software using a routine that applies the Span&Wagner equation of state (EoS) based on NIST database for any thermodynamic point defined by pressure and temperature.

PERFORMANCE COMPARISON EXPECTED VS TEST

The test was an ASME PTC-10 Type I test, hence executed under conditions equal to the design (e.g., gas composition and inlet total temperature & pressure). The goal was to measure the compressor performance and plot the relevant curves.
Performance test has been executed with the following gas and conditions

- GAS: CO_2
- Suction Total Pressure: 79.79 bar A
- Suction Total Temperature: 306.15 K
- 100% speed: 11400 RPM

Inlet conditions have been kept quite close to design values. Expected performance and test results have been evaluated with Span&Wagner EoS based on NIST database. Regarding design values, an illustration of deviations is given in the FIGURE 5, where moving from right to left limit the deviations for suction temperature and pressure are in the range ±1%.

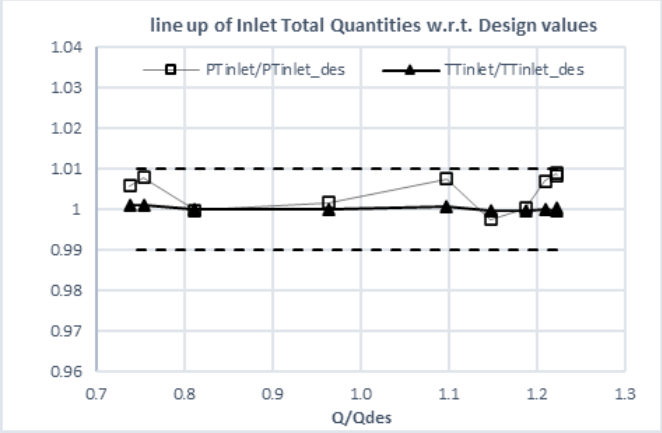

Figure 5: Variation of inlet pressure and temperature during exploration of 100% speed curve

Table 1: Summary table at design point

Parameter		Design condition	Test condition	Deviation test/design [%]
Suction Pressure	[bar-A]	79.79	79.9	0.17
Suction Temperature	[°C]	33°	33.03	0.1
Suction Volume Flow	[m3/h]	1029.9	1029.9	0
Speed	[-]	11400	11405	0.05

The test campaign can be divided into two main sections:

1. Early test commissioning
   - performance test far from critical point
   - performance test on a series of single points to set-up the best strategy to approach design point
2. Design point performance (complete curve exploration from right to left limit)
   - 100% speed at 0° IGV pre-rotation
   - Impact of IGV and speed
   - Sensitivity varying inlet pressure and temperature at design speed and IGV 0°

Early test commissioning was performed to set-up the best strategy to approach design point and pass through the high-gradients region in proximity to the critical entropy value. Then design point performance (complete curve exploration from right to left limit) have been assessed and measured, with exploration of off design conditions and impact of IGV pre-rotation.

Early Test commissioning

In the first part of commissioning the machine operated far from critical point where thermodynamic quantities are characterized by properties for which the ideal gas model is still a good approximation of gas behavior (Figure 6). The rotating speed has been set to guarantee the similitude in terms of inlet flow coefficient.

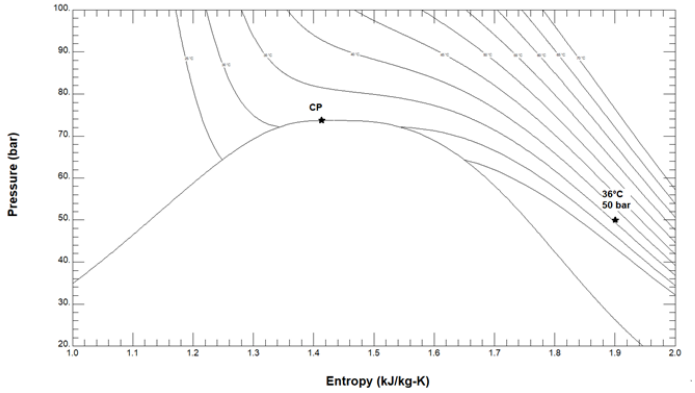

RPM: 8625
PT: 50 bar-A
TT: 36°C
Gas: 100% CO2

Figure 6: Inlet conditions on Entropy-Pressure plot for performance far from critical point

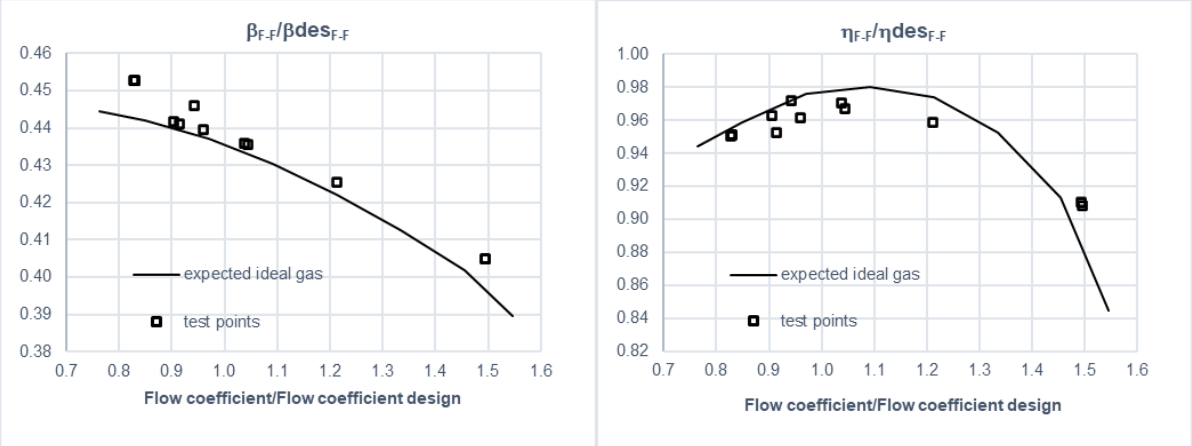

Figure 7: Normalized pressure ratio and efficiency curves far from critical point

The results are in good agreement with experimental data confirming that in these conditions, where inlet pressure and temperature are very far from critical point (CP), the assumption of considering ideal gas properties is a proper choice to predict performance (Figure 7). Once completed the test far from CP a series of single points (positioned close to the design volume flow) have been run to study the best way to approach critical point moving from right of critical entropy, passing it and hence moving towards design inlet conditions. During this procedure the performance measurements have been stabilized point by point to see the envelop in terms of pressure ratio and power. The results are given in the Figure 8. It can be highlighted that, starting from points far from CP where entropy is higher than the critical one and progressively moving the inlet conditions close to the design one the pressure ratio increases with the power (as expected) but close to the design, even if the flow coefficient remains quite constant (triangles dots), due to the decreasing compressibility the pressure ratio (solid circle) increases while the power remains flat (squares). This evidence is in good agreement with the expectations, proving that running close to CP gives benefits in terms of compression work and hence overall cycle efficiency.

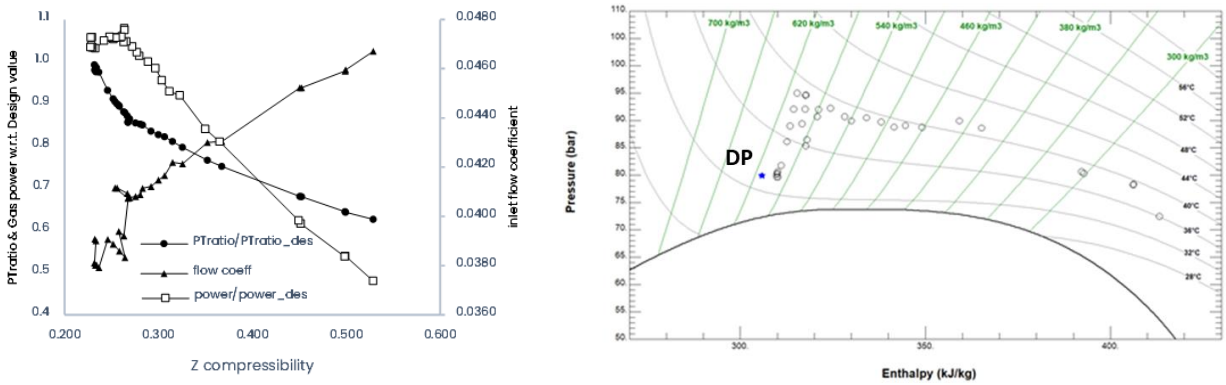

Figure 8: Points line-up showing the path used to approach the operation at design point

Design point performance

On the following pages summary results for the cases at design condition with open IGV (0°deg) and closed IGV (-25° and -50°) are shown. Figure 9 shows the results for design condition and 100% speed compared with expected. The expected are calculated using a novel method developed in collaboration with Politecnico di Milano, shown in [1] and [11], that considers the CO_2 real gas behavior close to CP with coexistence of gas and liquid phases. As seen in the previous paragraph in the sCO_2 cycle the compressors take advantages from the real gas behavior of the working fluid near the critical point, but the consequent large variation of CO_2 properties may have technological implications on the design of turbomachinery and more specifically on compressor first impeller. The oncoming flow is close to saturation line, accelerates around the blade leading edge with a local expansion and static pressure decreases approaching the region of large gradient promoting phase-change phenomena with coexistence of cavitation phenomena and compressibility effects. Speed of sound may drop significantly producing sudden increase of local Mach number. In this condition shock waves may occur, with direct implications on operating range and efficiency. As showed in Figure 8 the novel method proposed matches quite good the prediction of right limit that is located close to 120% of design flow, and the shape of curve for pressure ratio (β) and polytropic efficiency (η) are well predicted with minor deviation with respect to expected.

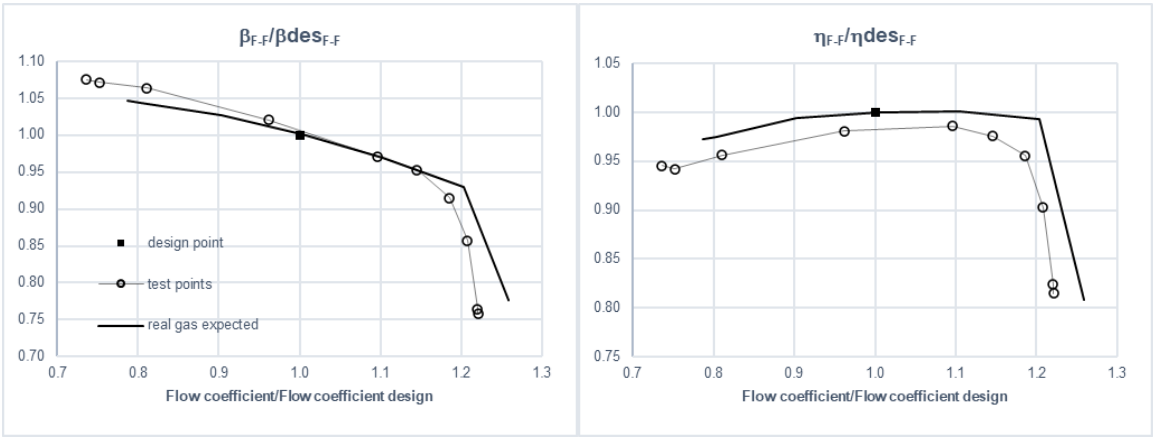

Figure 9: Normalized pressure ratio and efficiency curves at 100% speed and no pre-rotation from IGV

In Figure 10 the results with IGV angles ranging from +10° to -50° are given together with performance curves at closed IGV and reduced speed (60% and 80%) to verify the minimum operating flow that the machine can handle and the corresponding pressure ratio.

It can also be observed that, acting on IGV positions from 0° to -50°, the design flow can be reduced by 20% keeping the design value of pressure ratio (β), with a corresponding decrease of compression efficiency (η) by about 6% with respect to design value.

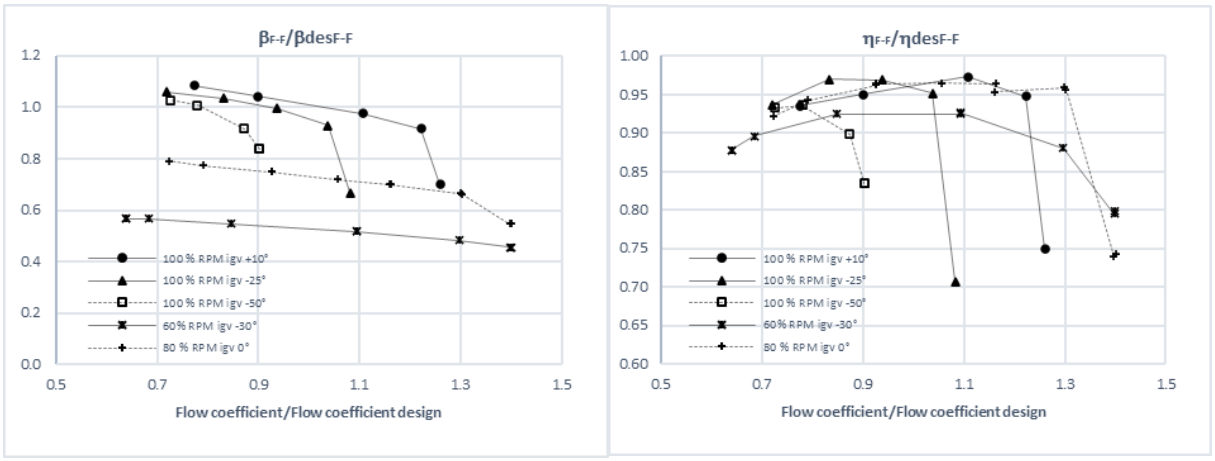

Figure 10: IGV impact on normalized pressure ratio and efficiency curves at 100%, 80% and 60%speed

DOE on Inlet Pressure & Temperature

Once completed the performance curves at design condition a small design of experiments (DOE) have been done varying the inlet conditions (Pressure and Temperature) and hence investigating the impact of margin to saturation line at compressor inlet (Table 2).

Table 2: Thermodynamic conditions for DOE points

condition	**RPM**	**Pin[bar]**	**Tin[°C]**
design	11000	79.8	33
Opt#1	11000	79.8	31
Opt#2	11000	79.8	34.5
Opt#3	11000	79.8	36
Opt#4	11000	75.6	31

This DOE has been useful to highlight performance sensitivity with respect to inlet conditions. In Figure 11 the results are given for performance obtained varying only inlet temperature while keeping inlet pressure to design value (79.8 bar) while in Figure 12 the results are given for a concurrent decreasing of both pressure and temperature. In general, it is notable that the margin to saturation line strongly affects performance, in fact when the combination of inlet temperature and pressure leads in a region characterized by lower thermodynamic gradients the margin with respect to saturation line is increased with beneficial impact on compressor operability. On the contrary, when the margin to saturation is decreased (Figure 12, 75.6 bar and 31°) the choke limit is further anticipated with respect to the design curve and in this specific case it is located quite close to design flow (Q/Qdes=1), significantly reducing the operating range and the possibility to correctly operate the machine.

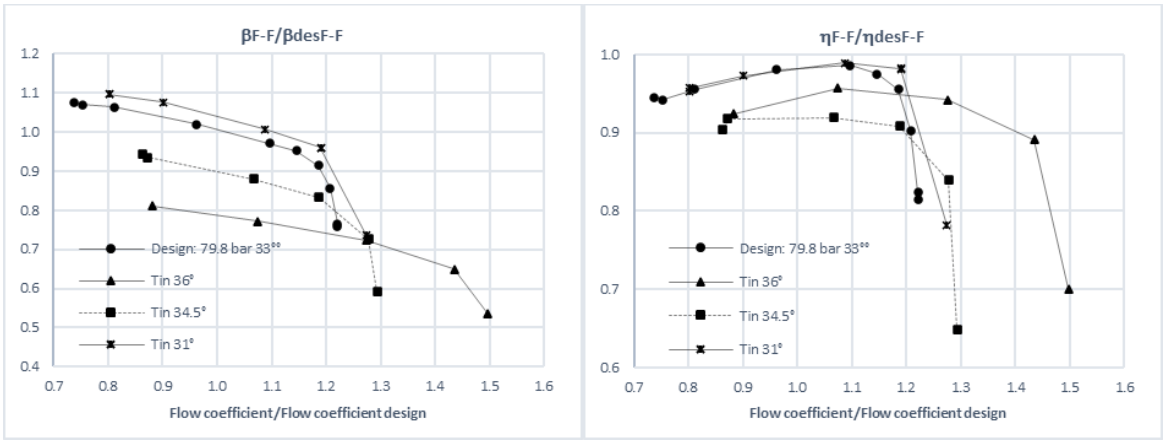

Figure 11: Normalized pressure ratio and efficiency curves with inlet conditions at higher margin to saturation line

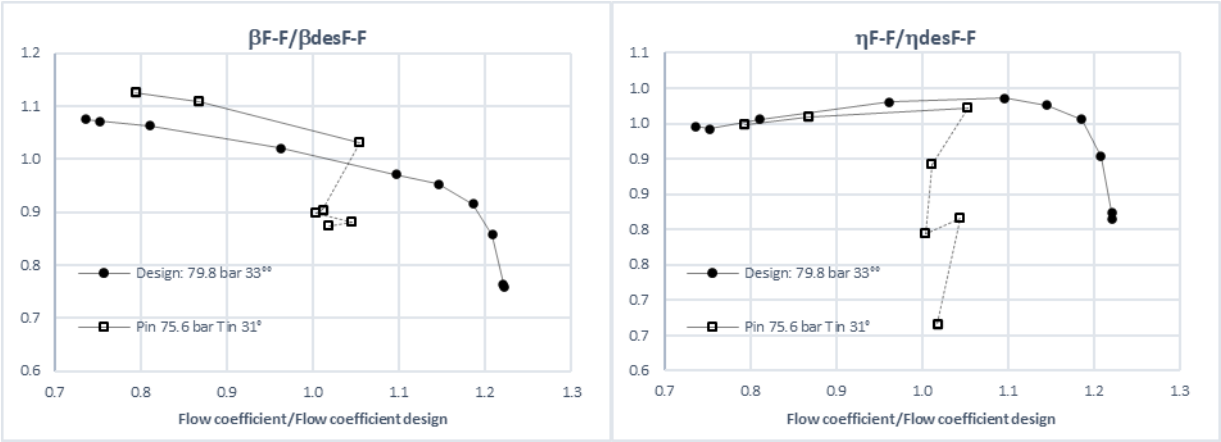

Figure 12: Normalized pressure ratio and efficiency curves with inlet conditions at lower margin to saturation line. Choking region in dashed line

ROTORDYNAMICS

From a rotordynamic standpoint, these peculiar operating conditions introduced new challenges. Looking at the API617 reference diagram [7], see Figure 13, the compressor representative point falls in a region well beyond the safe zone due to the very high density. So, a detailed stability rotordynamic analysis is required where all the potential destabilizing sources are included (Level 2).

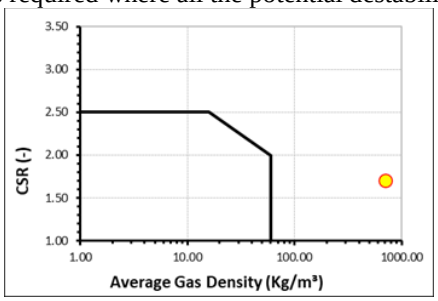

Figure 13: API stability reference diagram

Rotor was stacked type: two stages and two shaft ends. The rotor balancing activity was carried out with a special focus on repeatability. This is because the rotor needed to be disassembled after the balancing for the final assembly in the casing. This is not the first time for the Authors Company to build a stacked rotor in general but in the past the mechanical centering among the shaft parts was based on the Hirth coupling while for this specific case the parts are joined through simple butt joints. For this reason, after performing the high-speed balancing the rotor came back to the workshop for a complete disassembly and reassembly. Then the rotor was installed again in the bunker for vibrations measurements. Measured vibrations were compared with either the original vibrations (before any balancing) and the vibrations from the high-speed balancing. As it is shown in the Figure 14, vibrations showed a satisfactory level of repeatability, and they were much lower than at the original state. This means the assembly mechanical tolerances were precise enough to guarantee the balancing quality repeatability.

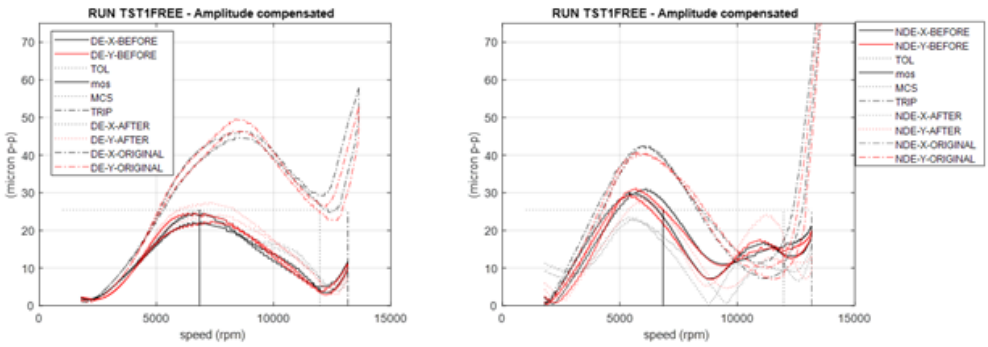

Figure 14: Rotor vibration comparison

The rotor was then subjected to a dedicated ping test to check the proper rotordynamic modelization since the novelty of the butt joint technology. The comparison between predictions and measured frequencies showed a significant discrepancy at the beginning (especially on the first bending mode). The gap was finally reduced through a model fine tuning which led to the good match shown in the Table 3. All the details of the ping test measurements and model fine tuning will be subject of a dedicated paper, so they are not described here.

Table 3: Experiments vs. Predictions

	CASE_B TUNED INNER ONLY TUNED Predicted NF Hz	Measured NF Hz	DELTA %
1st mode Main Rotor	159	158.6	0%
		158.9	0%
2nd mode Main Rotor	462	453.1	-2%
		457.5	-1%
		457.9	-1%
1st mode Tierod	263	257.3	-2%
		257.4	-2%

Based on the updated model, the final rotordynamic analysis was performed. Journal bearings are tilting pad, 5pad, Load on Pad configuration. Clearance is in the range 1.6-2/1000. These bearings are also equipped with Integral Squeeze Film Damper (ISFD) to improve the damping capability as already shown in [2]. The first three rotor modes are expected to be critically damped (AF< 2.5 according to API617): the first and second mode are rigid modes at relatively low frequencies while the third mode is expected to fall within operating speed range. The tie-rod mode is expected to be fully separated from maximum continuous speed (MCS). Modelization is also based on actual bearing clearance and considers integral squeezed film damper (ISFD) properties, see Table 4.

Table 4: Rotordynamic analysis summary

ACTUAL BRG CLEARANCE		Rotor modelization tuned on ping test			
Note	**NF**	**Log Dec**	**AF**	**Sma**	**Smr**
-	rpm	-	-	-	-
NF1	2031	5.62	0.6	70%	35%
NF2	3068	9.17	0.34	55%	32%
NF3	8364	2.86	1.1	-22%	NA
Tie-rod	15478	0.06	49.5	29%	27%

Stability analysis was also performed, considering the actual seals geometry and relevant clearances. Worth noting here is the presence of a pocket damper seal as a balance piston seal, following the satisfactory outcomes shown in [3]. The API Level 2 analysis showed log dec values much higher than 1 for the first forward mode and they will be discussed in a dedicated paper. After the balancing process, the rotor, as anticipated, was disassembled for the final assembly in the compressor bundle. Even if the repeatability check done in the bunker was promising the probability to have high vibrations at the first run was still high. This was because the whole job coupling was installed for the first time on the drive end side (balancing was performed using the job hub only) and because of the eventual impact of the other equipment in the train (GE 10 gas turbine and parallel axes gearbox). A field balancing (using only the coupling hub plane) was needed to tweak vibrations within acceptable limits (e.g., 30micron). Finally, the Full Load Full String test was performed, and the rotor always showed a satisfactory rotordynamic behavior. As an example, Figure 15 show the Bode plots for a startup from settling out pressure (SOP) @100bara and Figure 16 a waterfall plot reflecting a full test day.

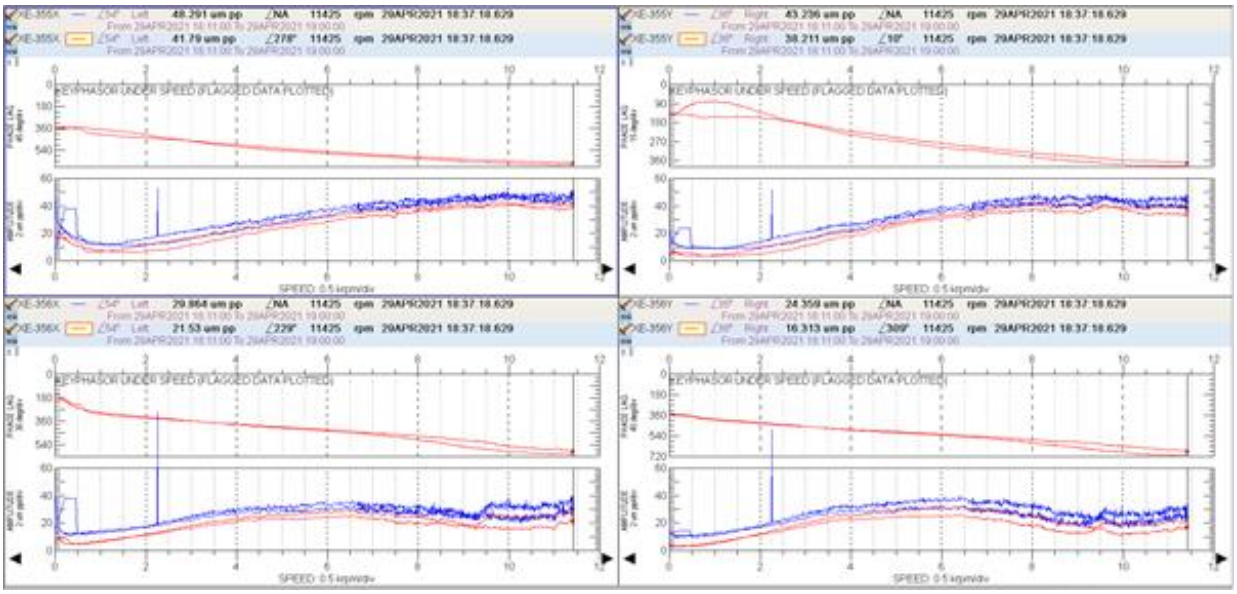

Figure 15: Bode plots relevant to a startup from SOP

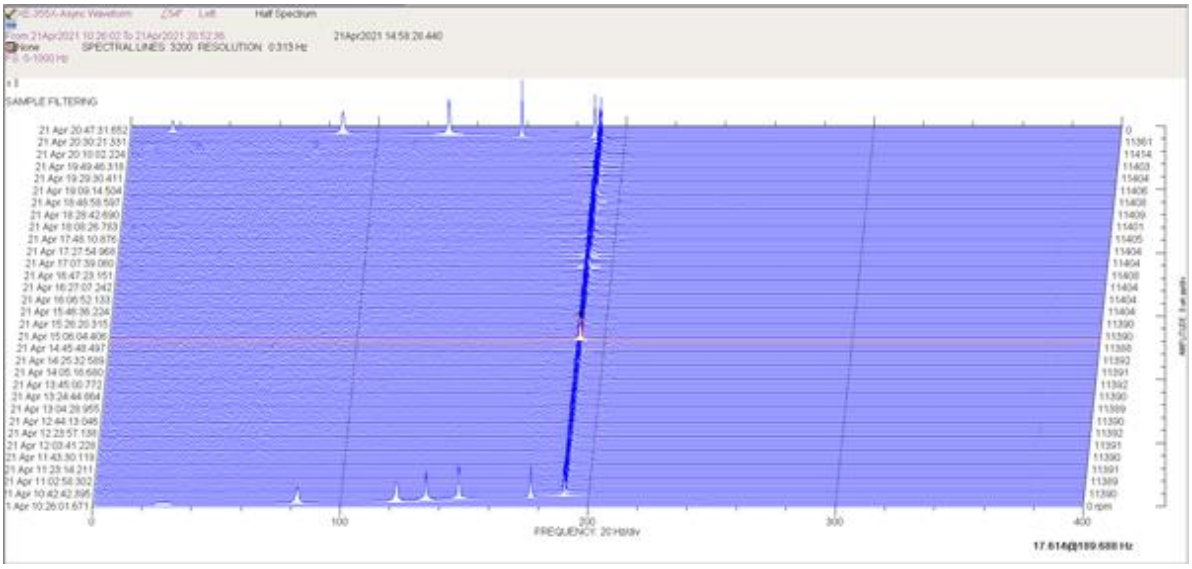

Figure 16: Waterfall plot relevant to a full test day

Figure 16 especially is confirming the high level of stability predicted at design stage. High frequency vibration data were of course recorded all through the test duration and later analyzed through the OMA approach. Due to the extremely high damping level, it was not possible to clearly identify either the rotor first forward mode or other modes within the running frequency range. These details about stability, both theoretical and experimental, will be also part of a dedicated paper and they are not discussed in depth at this stage.

AXIAL THRUST

The thrust calculation is performed through the following equation as described in [5]:

$$T=T_I+T_{II}+T_b+T_m+T_c$$

T_I is the primary effect given by the differential pressure seen by the impeller considering a constant pressure distribution (impeller suction pressure at the inlet and impeller discharge pressure on shroud and hub). T_{II} is the secondary effect due to the difference of the actual pressure distribution on the surface of the impeller and the primary effect. The actual pressure distribution in the cavity impeller-

diaphragm is generated by the leakage flow and the radial gradient of the pressure due to the rotation. T_b is the component of the axial thrust due to the differential pressure across the balance drum. T_m is the component of the axial thrust on the rotor generated by the axial momentum variation of the gas flow from the inlet to the exit of the impeller. Finally, T_c is the component of the axial thrust given by the coupling.

The axial thrust calculation in a centrifugal compressor is often affected by several uncertainties and the results may differ from the actual value for many reasons. The thrust bearing is then selected to have large margin, often much higher than the 50% margin of the bearing ultimate load rating at the specified operating conditions required by API617 [7]. A contribution to the uncertainty of the calculation result may come from the geometrical tolerance which drives the leakage across the seal and consequently the pressure distribution. The uncertainty in the calculation of the T_I is mainly related to the error in evaluating the inlet and discharge pressure of each stage and to the chosen manufacturing tolerance interval. The inlet and outlet pressures are usually well predicted in the design phase and during the operation may also be measured by installing dedicated instrumentation probes. The geometrical data can be measured during the manufacturing phase, removing the variability introduced during the design. This leads to state that primary effect uncertainty is limited. Almost same consideration can be stated for the other components of the axial thrust T_b, T_m, and T_c. The major source of uncertainties in the calculation comes then from the secondary effect $T_{//}$ which requires the tuning of the core rotation coefficient k [5], according to experiments. Available data for k are nevertheless far from the one encountered with sCO_2 condition, and their extrapolation may lead to a consistent error. For this reason, to avoid undesirable poor axial thrust capability, the thrust bearing was selected with a large margin with respect to the maximum axial load expected in the design phase and equipped with load cells to allow axial thrust measurements. In Figure 17 it is possible to capture the computational error extrapolating the data for CO_2 in gas condition, comparing expected thrust (Tnet design) with measured data (Tmeasured). Tuning the core rotational coefficient k leads to a calculated thrust (Tnet corr) more aligned with measured data.

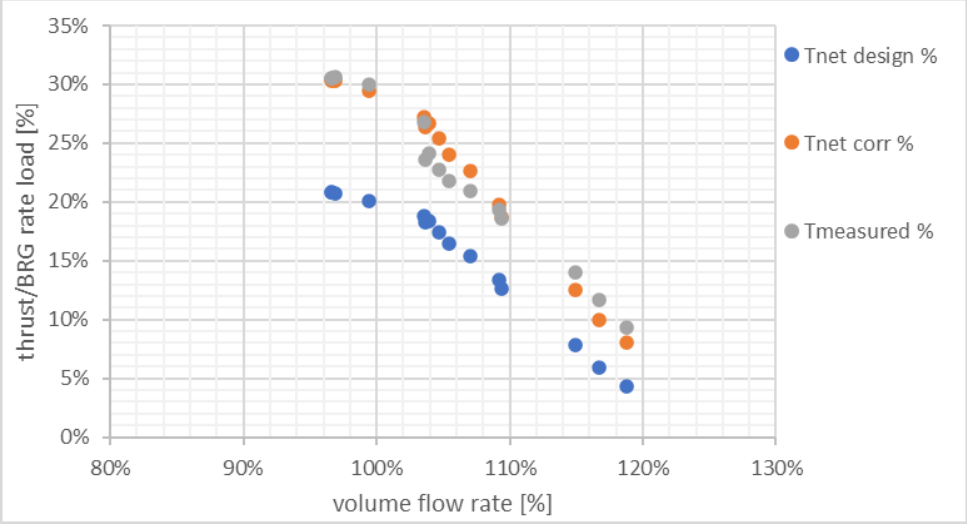

Figure 17: Thrust vs flow rate

CONCLUSION

All over the test period, 125hrs running in CO_2 supercritical conditions, prototype compressor performed very well, showing a stable rotordynamic behavior and acceptable axial load. Compressor operated at a speed varying from 60% to 100% and IGV position from +10° to -50°. In addition to the performance curve measurements carried out with compressor suction pressure and temperature as per design conditions, compressor operated also in some off-design conditions, where CO_2 thermodynamic conditions were significantly different. The main goal was to evaluate compressor behavior in case of unexpected problems of the loop suction compressor control or possible transient conditions that may arise during operation. Compressor operated up to a maximum suction density of 685 kg/m3 and up to an absorbed compressor power equal to 8285 kW.

Compressor behavior was satisfactory on all design and tested off-design conditions. Nevertheless, also confirmed critical operability in the region of high thermodynamic property gradients. This area was known since the beginning of the project as a possible critical area for operating the compressor. As a matter of fact, compressor design point was selected close to this area, to exploit the advantage of a great reduction in compressor absorbed power, but at the same time far enough to allow a smooth control of the unit. For

this reason, OEM recommend avoiding continuous operating in that area. Figure 18 shows the off-design range explored during the prototype test campaign in light green and in the dark green the most critical area for stable operation.

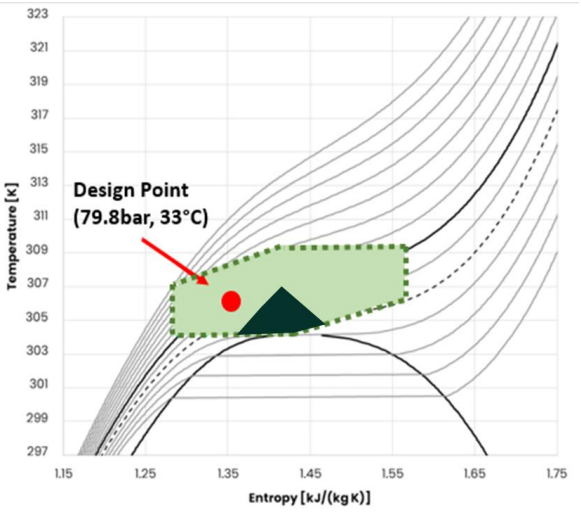

Figure 18: Range of off-design conditions tested

NOMENCLATURE

k = core rotation coefficient (-)
T = axial thrust (M L T-^{2})
T_I = primary effect component (M L T-2)
T_{II} = secondary effect component (M L T-^{2})
T_b = balance piston component (M L T-^{2})
T_m = variation of gas momentum component (M L T-2)
T_c = coupling component (M L T-2)

CP = Critical Point
DGS = Dry Gas Seal
DOE = Design of Experiment
EM = Electric Motor
EoS = Equation of State
EU = European Union
GB = Gear Box
IGV = Inlet Guide Vanes
ISFD = Integral Squeezed Film Damper
MCS = Maximum Continuous Speed
OEM = Original Equipment Manufacturer
OMA = Operating Modal Analysis-
sCO_2 = Super Critical Carbon Dioxide
SOP = Settling Out Pressure
TOR = Teeth on rotor

FIGURES

REFERENCES

[1] Giacomo Persico, Paolo Gaetani, Alessandro Romei, Lorenzo Toni, Ernani Fulvio Bellobuono, Roberto Valente, Implications of Phase Change on the Aerodynamics of Centrifugal Compressors for Supercritical Carbon Dioxide Applications, 2021, https://doi.org/10.1115/1.4049924

[2] Vannini Giuseppe, Pelagotti Antonio, Rizzo Emanuele and Carmicino Carmine. "Rotordynamic Test Results from a High Flexibility Ratio-High Pressure Fully Instrumented Centrifugal Compressor Test Vehicle." Proceedings of the 46th Turbomachinery Symposium, Houston, TX, 2017. DOI http://hdl.handle.net/1969.1/166802.

[3] Milani A., Scarbolo L., Bigi M., Rizzo E., Evangelisti S., Borghesi M. V., Vannini G. Sassanelli G., "Performance test of a Full Size Wet Tolerant Compressor" – Proceedings of ATPS 2021, Virtual Event.

[4] Childs D., Elrod D., and Hale. K., 1988, A Rotordynamic Coefficient and Leakage Test Results for Interlock and Tooth-on-Stator Labyrinth Seals, @ ASME Paper Number 88-GT-87, Gas Turbine Conference.

[5] Baldassarre L., Bernocchi A., Fontana M., Maiuolo F., Rizzo E., Axial Thrust in High Pressure Centrifugal Compressors: Description of a Calculation Model Validated by Experimental Data from Full Load Test – 44th Turbomachinery Symposia

[6] Elicio G., Annese F., Experimental approach to predict the residual axial thrust in centrifugal pumps, Proceedings of the ASME-JSME-KSME 2019 Joint Fluids Engineering Conference

[7] API 617, 2014, "Axial and Centrifugal Compressors and Expander-Compressors," Eighth Edition, American Petroleum Institute, Washington, D.C

[8] D1.3 - Report on the selected cycle architecture, https://www.sco2-flex.eu/wp-content/uploads/2019/06/D1.3-%E2%80%93-Report-on-the-selected-cycle.pdf

[9] Lemmon, E. W., McLinden, M. O., and Huber, M. L.,2002. NIST standard reference database 23: Reference fluid thermodynamic and transport properties-REFPROP, version 8.0. Tech. rep., National Institute of Standards and Technology, Standard Reference Data Program, Gaithersburg

[10] Simple contact stiffness model validation for the tie bolt rotor design with butt joints and pilot fits, GT2019-90396, Aaron M. Rimpel, Matthew Leopard, Proceedings of ASME Turbo Expo 2019

[11] Experimental and Numerical Performance Survey of a MW-Scale Supercritical CO2 Compressor Operating in Near-Critical Conditions, F.Bellobuono, L.Toni, R.Valente, G.Persico, A.Romei, P.Gaetani, sCO2 Symposium, San Antonio Texas Feb 2022

ACKNOWLEDGEMENTS

The authors gratefully acknowledge all sCO2Flex project partners for their active participation in the joint Horizon 2020 Program which included the test campaign reported in the present paper